

Supplementary Information

Methylxanthines for Halogen Bonded Cocrystals with 1,4-Diiodotetrafluorobenzene: Green Synthesis, Structure, Photophysics and DFT Studies

Mónica Benito,^{1*} Rosario Núñez,^{1*} Sohini Sinha,¹ Claudio Roscini,² Yoan Hidalgo-Rosa,^{3,4}
Eduardo Schott,³ Ximena Zarate,^{5*} Elies Molins¹

¹Institut de Ciència de Materials de Barcelona (ICMAB-CSIC), Campus UAB, 08193 Bellaterra, Spain

²Catalan Institute of Nanoscience and Nanotechnology (ICN2), CSIC and The Barcelona Institute of Science and Technology (BIST), Campus UAB, Bellaterra, Barcelona 08193, Spain

³Departamento de Química Inorgánica, Facultad de Química y Farmacia, Centro de Energía UC, Centro de Investigación en Nanotecnología y Materiales Avanzados CIEN-UC, Pontificia Universidad Católica de Chile, Avenida Vicuña Mackenna, 4860 Santiago, Chile

⁴Facultad de Ingeniería, Universidad Finis Terrae, Av. Pedro de Valdivia 1509, Providencia, Santiago, Chile

⁵Instituto de Ciencias Aplicadas, Facultad de Ingeniería, Universidad Autónoma de Chile, Av. Pedro de Valdivia 425, Santiago, Chile

TABLE OF CONTENTS

Figure/Table	
Figure S1	Structural models used in the simulations: a) cocrystals and b) Free xanthines.
Table S1	Hydrogen-bond geometry (Å, °) for compounds CAF-DITFB , TPH-DITFB and TBR-DITFB (2:1) .
Figure S2	TGA-DSC of the cocrystal CAF-DITFB .
Figure S3	a) TGA-DSC trace of cocrystal TPH-DITFB and b) phase transformation between theophylline and cocrystal TPH-DITFB .
Figures S4	Transformation process by heating CAF-DITFB cocrystal (left) to CAF (right). Optical images under visible light (a and b) and under UV (365 nm) (c and d). Under UV the off-on transformation could be observed.
Figures S5	FTIR spectra of natural xanthines, coformer DITFB and their cocrystals.
Table S2	Summary of characteristic vibrational modes of the studied xanthines and coformer DITFB .
Figures S6	Absorption and fluorescent emission spectra of TPH and TPH-DITFB cocrystal (a and b).
Table S3	Comparison of experimental and theoretical calculated cell parameters.
Table S4	X-bond interaction with distances and angles for the optimized cocrystals through periodic DFT calculations

Table S5	Surfaces of the molecular orbital (MOs) with their energies (eV), PBE0/def2-TZPP theoretical level.
Figure S7	Energy diagrams for the most probable emission pathways in free xanthenes. ISC, intersystem crossing.
Figure S8	Frontier molecular orbitals of CAF based on the configurations of first electronic excited state. a. FMO of CAF in the S_1 electronic state. b. FMO of CAF in the T_1 electronic state. MO involved in these emissive states of the T_1 electronic state are dotted by green lines.
Figure S9	Frontier molecular orbitals of theobromine (TBR) based on the configurations of first electronic excited state. a. FMO of TBR in the S_1 electronic state. b. FMO of TBR in the T_1 electronic state. MO involved in these emissive states of the T_1 electronic state are dotted by green lines.
Figure S10	Frontier molecular orbitals of theophylline (TPH) based on the configurations of first electronic excited state. a. FMO of TPH in the S_1 electronic state. b. FMO of TPH in the T_1 electronic state. MO involved in these emissive states of the T_1 electronic state are dotted by green lines.
Figure S11	Frontier molecular orbitals of cocrystals based on the configurations of ground electronic excited state. a. FMO of CAF-DITFB in the S_0 electronic state. b. FMO of TPH-DITFB in the S_0 electronic state. c. FMO of TBR-DITFB in the S_0 electronic state.
Figure S12	Energy diagrams for the most probable emission pathways in cocrystals. ISC, intersystem crossing.
Figure S13	Frontier molecular orbitals of cocrystals CAF-DITFB based on the configurations of first electronic excited state. a. FMO of CAF-DITFB in the S_1 electronic state. b. FMO of CAF-DITFB in the T_1 electronic state. MO involved in these emissive states of the T_1 electronic state are dotted by green lines.
Figure S14	Frontier molecular orbitals of cocrystals TBR-DITFB based on the configurations of first electronic excited state. a. FMO of TBR-DITFB in the S_1 electronic state. b. FMO of TBR-DITFB in the T_1 electronic state. MO involved in these emissive states of the T_1 electronic state are dotted by green lines.
Figure S15	Frontier molecular orbitals of cocrystals TPH-DITFB based on the configurations of first electronic excited state. a. FMO of TPH-DITFB in the S_1 electronic state. b. FMO of TPH-DITFB in the T_1 electronic state. MO involved in these emissive states of the T_1 electronic state are dotted by green lines.

Figure S1. Structural models used in the simulations: a) cocrystals and b) Free xanthenes.

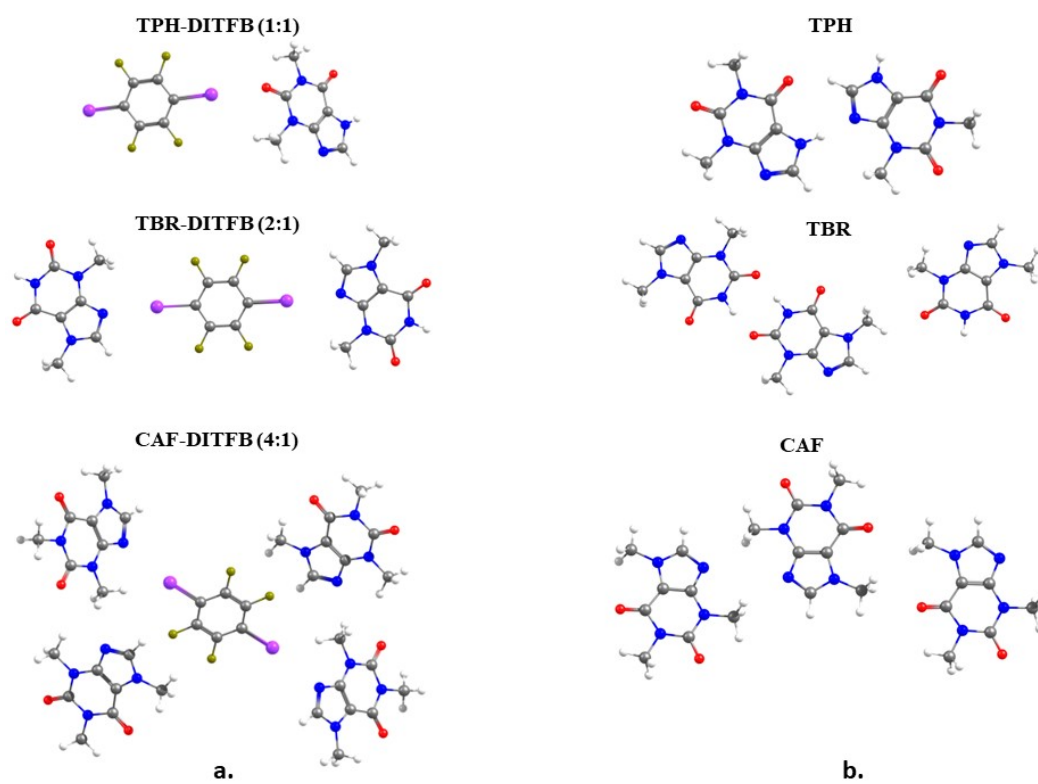


Table S1. Hydrogen-bond geometry (Å, °) for compounds **CAF-DITFB**, **TPH-DITFB** and **TBR-DITFB (2:1)**.

<i>Compound</i>	<i>D—H···A</i>	<i>D—H</i>	<i>H···A</i>	<i>D···A</i>	<i>D—H···A</i>
CAF-DITFB	C(14)-H(14C)···O(13)	0.96	2.48	3.097(13)	121.9
	C(28)-H(28)···O(11)#2	0.93	2.45	3.284(10)	149.6
	C(30)-H(30A)···O(31)#3	0.96	2.53	3.449(10)	161.4.0
	C(30)-H(30C)···O(31)#4	0.96	2.60	3.217(10)	122.2
	C(32)-H(32A)···I(1)	0.96	3.15	3.954(9)	141.9
	C(34)-H(34A)···O(11)#2	0.96	2.57	3.456(11)	153.1
TPH-DITFB	N(7)-H(7)···O(6) ⁱ	0.86	1.93	2.778 (4)	167.3
	C(1)-H(1A)···O(2) ⁱⁱ	0.96	2.53	3.425 (5)	155.9
	C(1)-H(1B)···O(2) ⁱⁱⁱ	0.96	2.63	3.227 (5)	120.4
	C(3)-H(3A)···I(1) ^{iv}	0.96	3.35	4.067 (4)	132.8
	C(3)-H(3B)···I(2) ^v	0.96	3.33	4.176 (4)	148.9
TBR-DITFB (2:1)	N(1)-H(1)...O(6)#1	0.86	2.03	2.887(6)	175.7
	C(7)-H(7A)...O(2)#2	0.96	2.31	3.245(8)	165.1
	C(7)-H(7C)...O(6)#3	0.96	2.63	3.544(8)	158.8

D-H: donor; A: acceptor

Symmetry codes for cocrystal **CAF-DITFB**: #1 -x+1,-y+2,-z+1 #2 -x+1,y+1/2,-z+3/2 #3 -x,y+1/2,-z+1/2 #4 -x,y-1/2,-z+1/2

cocrystal **TPH-DITFB**: (i) -x+1, -y+1, -z+2; (ii) -x+1/2, y-1/2, -z+3/2; (iii) -x+1/2, y+1/2, -z+3/2; (iv) x, y+1, z; (v) -x+1, -y+1, -z+1.

cocrystal **TBR-DITFB (2:1)**: #1 -x+1,-y+1,-z+2 #2 x-1,y-1,z #3 -x+1,-y,-z+2

Figure S2. TGA-DSC of the cocystal **CAF-DITFB**.

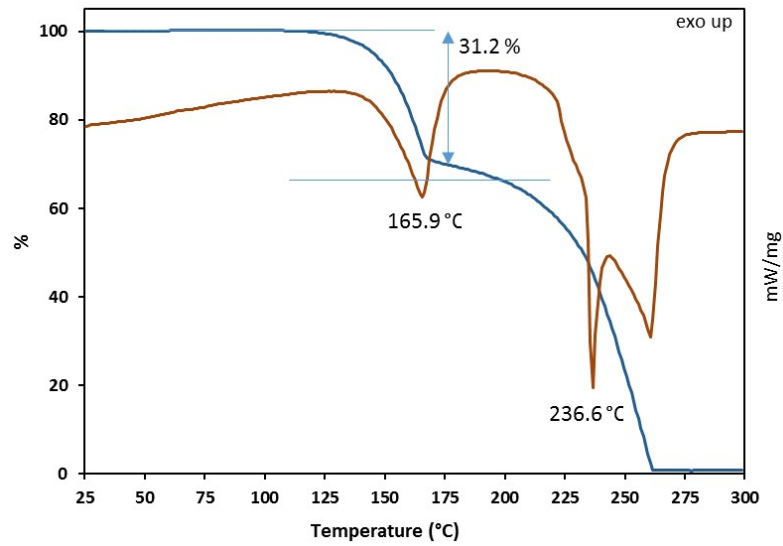


Figure S3. a) TGA-DSC trace of cocystal **TPH-DITFB** and b) phase transformation between theophylline and its cocystal.

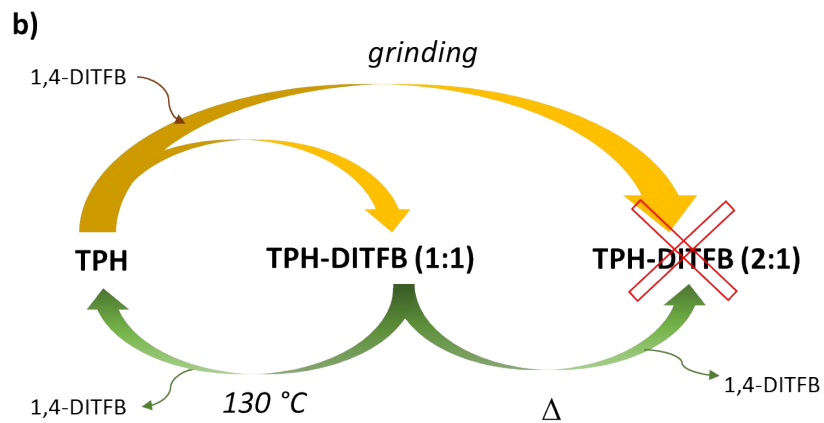
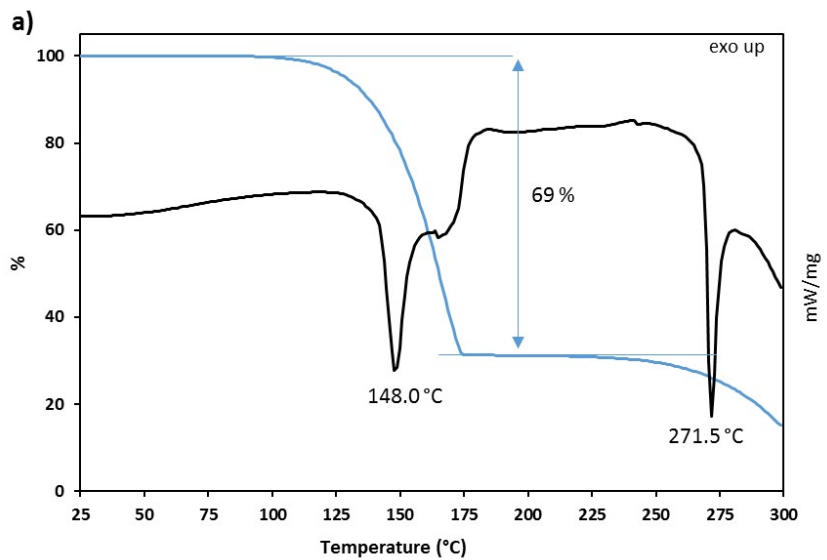
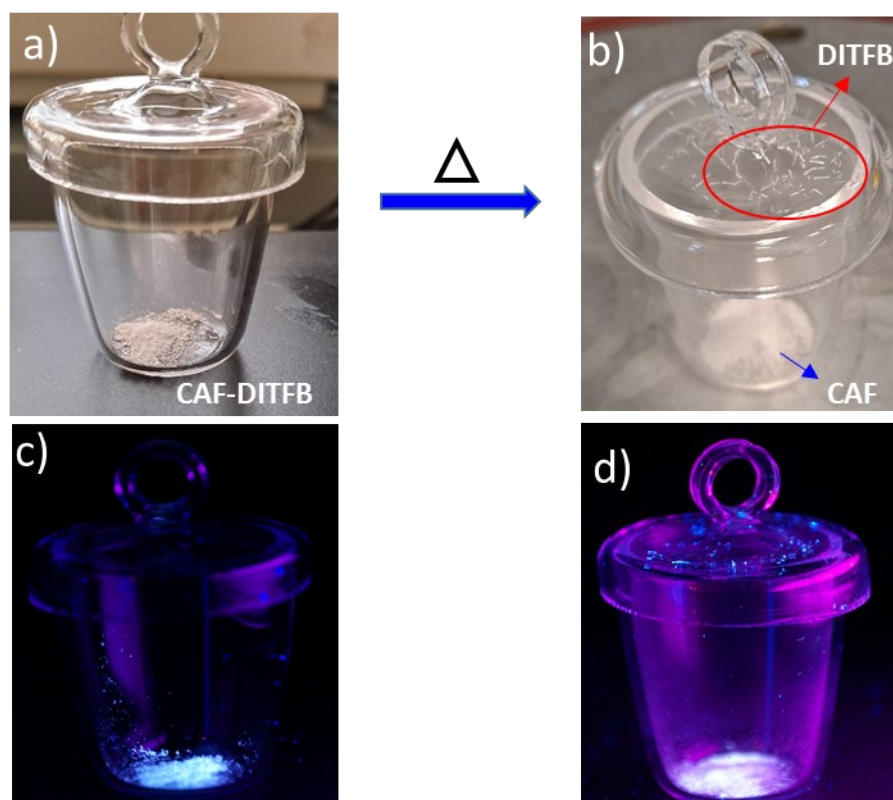
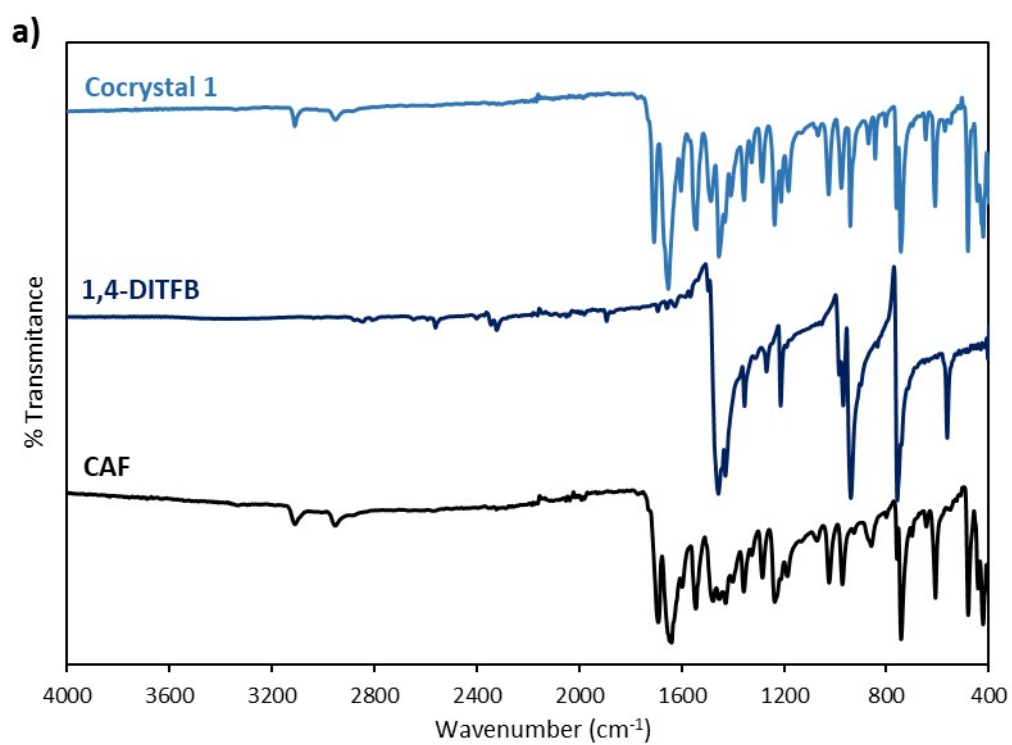


Figure S4. Transformation process by heating **CAF-DITFB** cocrystal (left) to **CAF** (right). Optical images under visible light (a and b) and under UV (365 nm) (c and d). Under UV the off-on transformation could be observed.



Figures S5. FTIR spectra of natural xanthines, coformer **DITFB** and their cocrystals.



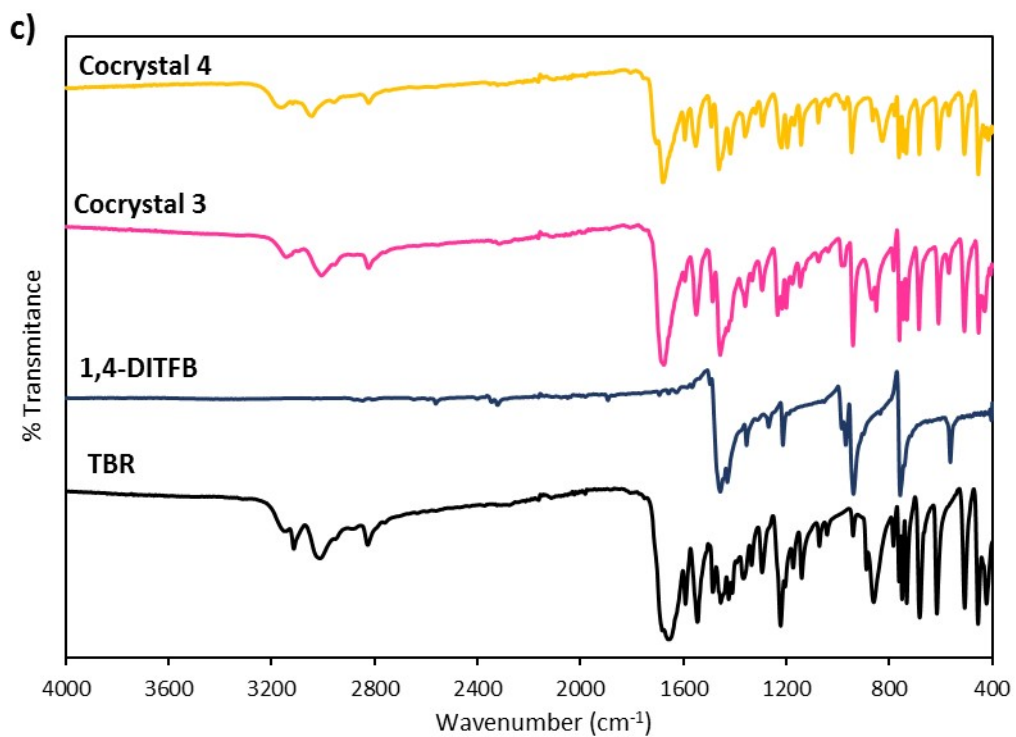
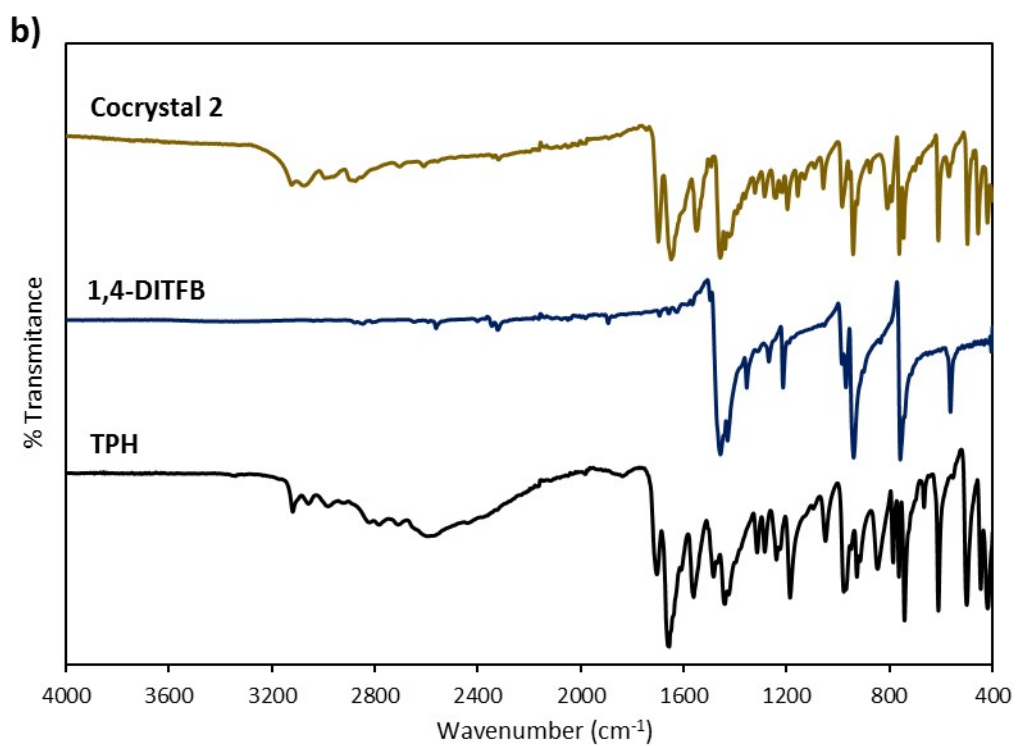


Table S2. Summary of characteristic vibrational modes of the studied xanthenes and cofomer **DITFB**.

Vibrational mode	DITFB	CAF	CAF-DITFB	TPH	TPH-DITFB	TBR	TBR-DITFB (1:1)	TBR-DITFB (2:1)
ν_{C-C} stretch	1456	-	1453	-	1458	-	1456	1461
ν_{C-F} stretch.	937	-	940	-	943	-	940	943
ν_{C-I} asymm.	755	-	743	-	761	-	758	761
$\nu_{C=O}; \nu_{C=N}$	-	1691; 1640	1707; 1651	1704; 1657	1699; 1645	1657; 1592	1675	1704; 1678
ν_{N-H}	-	3113; 2955	3113; 2950	3118;3 057; 2984	3123; 3075; 2998	3150; 3115; 3016; 2827	3139; 3005; 2824	3164; 3043; 2955; 2824

Figure S6. Absorption and fluorescent emission spectra of **TPH** and **TPH-DITFB** cocrystal (a and b).

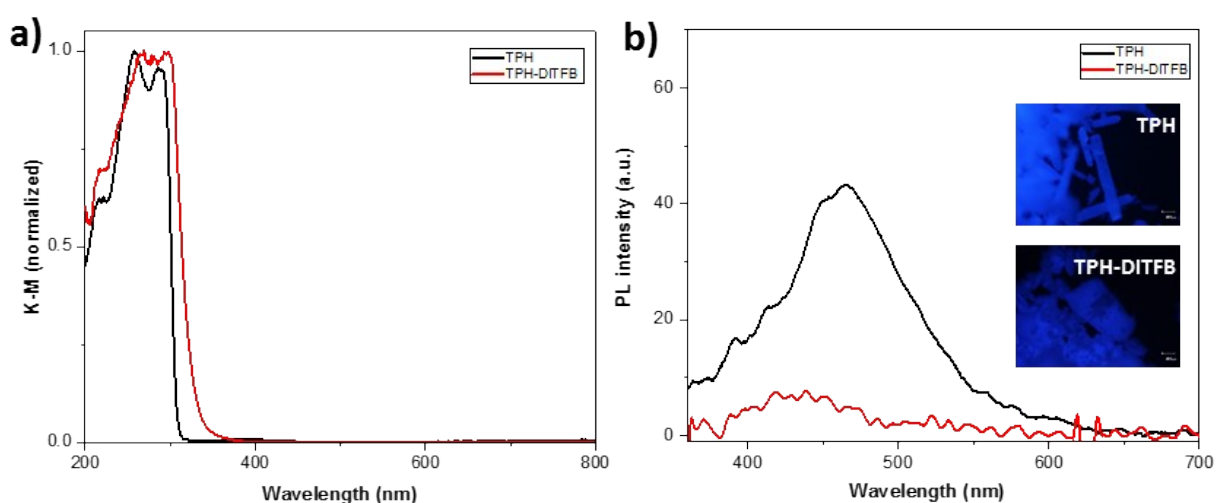


Table S3. Comparison of experimental and theoretical calculated cell parameters.

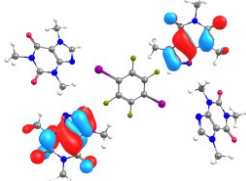
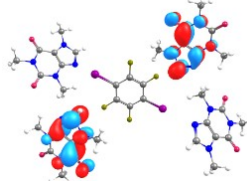
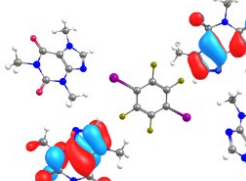
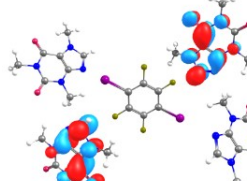
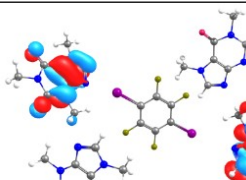
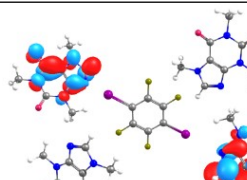
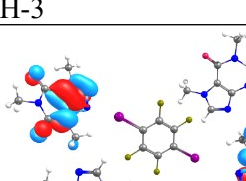
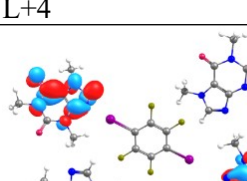
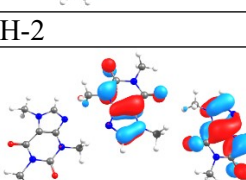
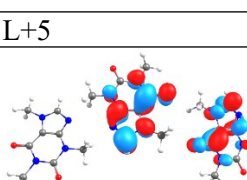
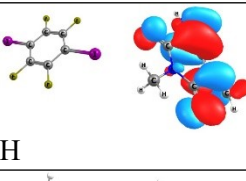
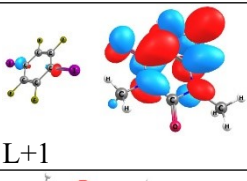
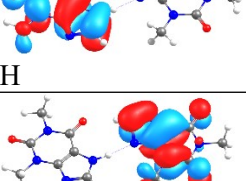
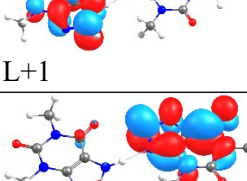
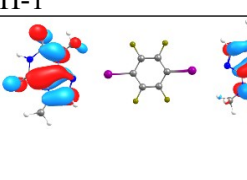
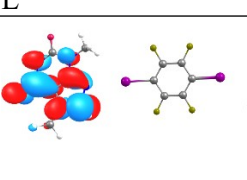


Parameters	CAF-DITFB		TPH-DITFB		TBR-DITFB (2:1)	
	Cryst data	Theo data	Cryst data	Theo data	Cryst data	Theo data
a (Å)	21.904(18)	21.924385	19.924(8)	19.821105	4.0269(18)	4.102633
b (Å)	4.044(4)	4.113429	4.4267(18)	4.451576	7.451(3)	7.422291
c (Å)	25.87(2)	25.756875	20.419(8)	20.357605	20.660(9)	20.589755
α (°)	90	90	90	90	82.022(8)	81.994578
β (°)	110.90(2)	110.996125	113.293(9)	113.367412	80.671(9)	80.634592
γ (°)	90	90	90	90	88.669(8)	88.664453

Table S4. X-bond interaction with distances and angles for the optimized cocrystals through periodic DFT calculations.

Cocrystal	I \cdots N	d(I \cdots N) (Å)	(C-I \cdots N) (°)
CAF-DITFB *	I(1) \cdots N(29)	2.859	175.41
CAF-DITFB (Periodic-DFT)	I \cdots N	2.803	174.40
TPH-DITFB*	I(1) \cdots N(9)	2.983	177.19
TPH-DITFB (Periodic-DFT)	I \cdots N	2.90	176.73
TBR-DITFB (2:1) *	I(9) \cdots N(9)	3.034	176.02
TBR-DITFB (Periodic-DFT)	I \cdots N	2.957	175.094

*Labeling of N and I atoms refer to the labeling of these atoms in the main text.

Table S5. Surfaces of the molecular orbital (MOs) with their energies (eV), PBE0/ def2-TZPP theoretical level.

System	$\lambda(\text{nm})$	f	Assignment	Active Molecular Orbital	
CAF-DITFB	257	0.32	$\pi^{(\text{CAF})} \rightarrow \pi^{*(\text{CAF})}$		
				H-1	L+6
	256	0.43	$\pi^{(\text{CAF})} \rightarrow \pi^{*(\text{CAF})}$		
				H	L+7
	256	0.43	$\pi^{(\text{CAF})} \rightarrow \pi^{*(\text{CAF})}$		
				H-3	L+4
	256	0.43	$\pi^{(\text{CAF})} \rightarrow \pi^{*(\text{CAF})}$		
				H-2	L+5
CAF	259	0.52	$\pi^{(\text{CAF})} \rightarrow \pi^{*(\text{CAF})}$		
				H-1	L
TPH-DITFB	249	0.29	$\pi^{(\text{TPH})} \rightarrow \pi^{*(\text{TPH})}$		
				H	L+1
TPH	255	0.23	$\pi^{(\text{TPH})} \rightarrow \pi^{*(\text{TPH})}$		
				H	L+1
	251	0.18	$\pi^{(\text{TPH})} \rightarrow \pi^{*(\text{TPH})}$		
				H-1	L
TBR-DITFB	255	0.67	$\pi^{(\text{TBR})} \rightarrow \pi^{*(\text{TBR})}$		
				H-1	L

			$\pi^{(\text{TBR})} \rightarrow \pi^{*(\text{TBR})}$	H-1	L
239	0.23	$\pi^{(\text{TBR})} \rightarrow \pi^{*(\text{TBR})}$	H	L+1	
TBR	251	0.14	$\pi^{(\text{TBR})} \rightarrow \pi^{*(\text{TBR})}$	H-1	L+1
	247	0.28	$\pi^{(\text{TBR})} \rightarrow \pi^{*(\text{TBR})}$	H-2	L
			H	L+2	

Figure S7. Energy diagrams for the most probable emission pathways in free xanthenes. ISC, intersystem crossing.

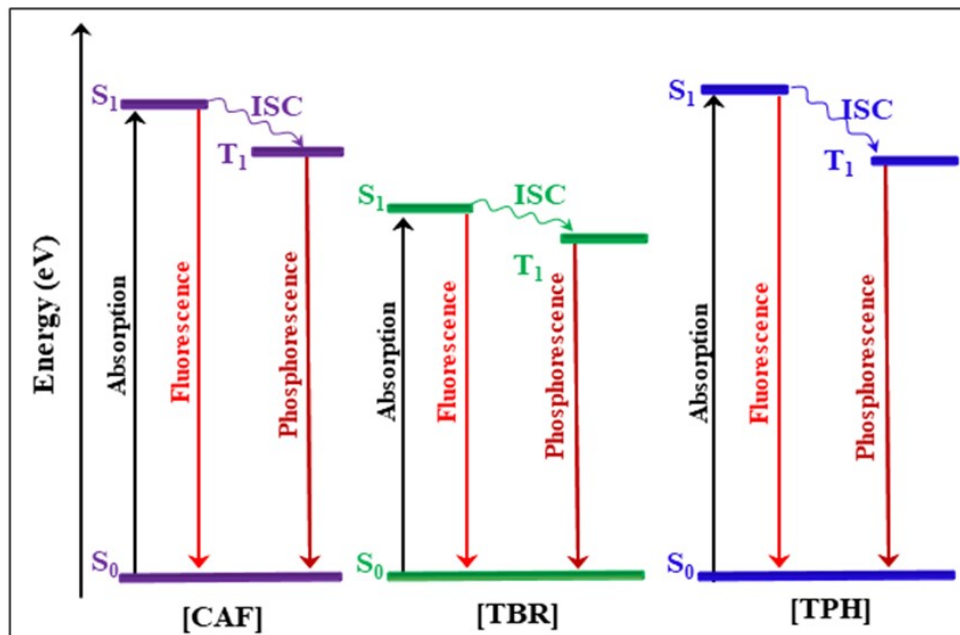


Figure S8. Frontier molecular orbitals of **CAF** based on the configurations of first electronic excited state. a. FMO of **CAF** in the S_1 electronic state. b. FMO of **CAF** in the T_1 electronic state. MO involved in these emissive states of the T_1 electronic state are dotted by green lines.

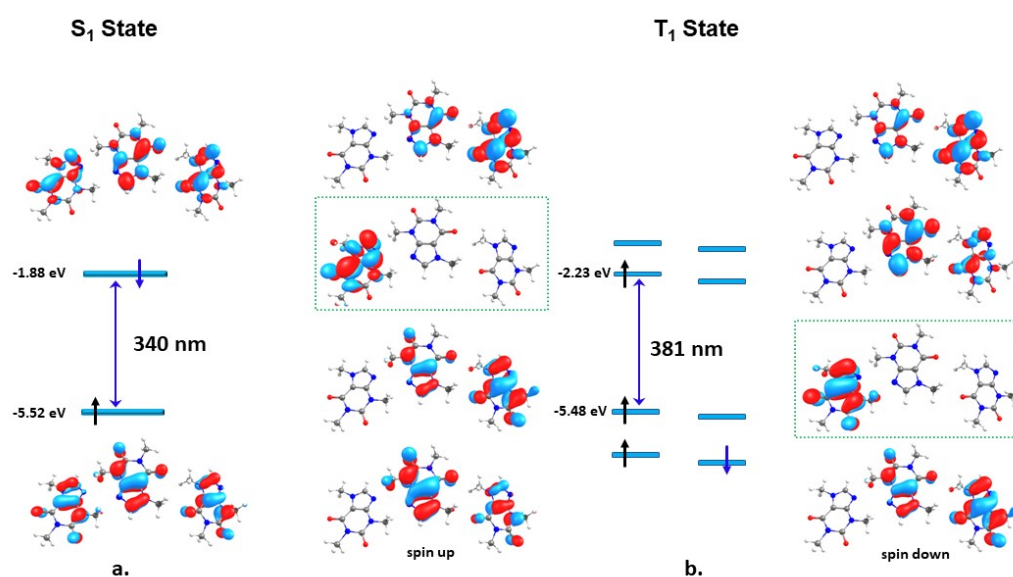


Figure S9. Frontier molecular orbitals of theobromine (**TBR**) based on the configurations of first electronic excited state. a. FMO of **TBR** in the S_1 electronic state. b. FMO of **TBR** in the T_1 electronic state. MO involved in these emissive states of the T_1 electronic state are dotted by green lines.

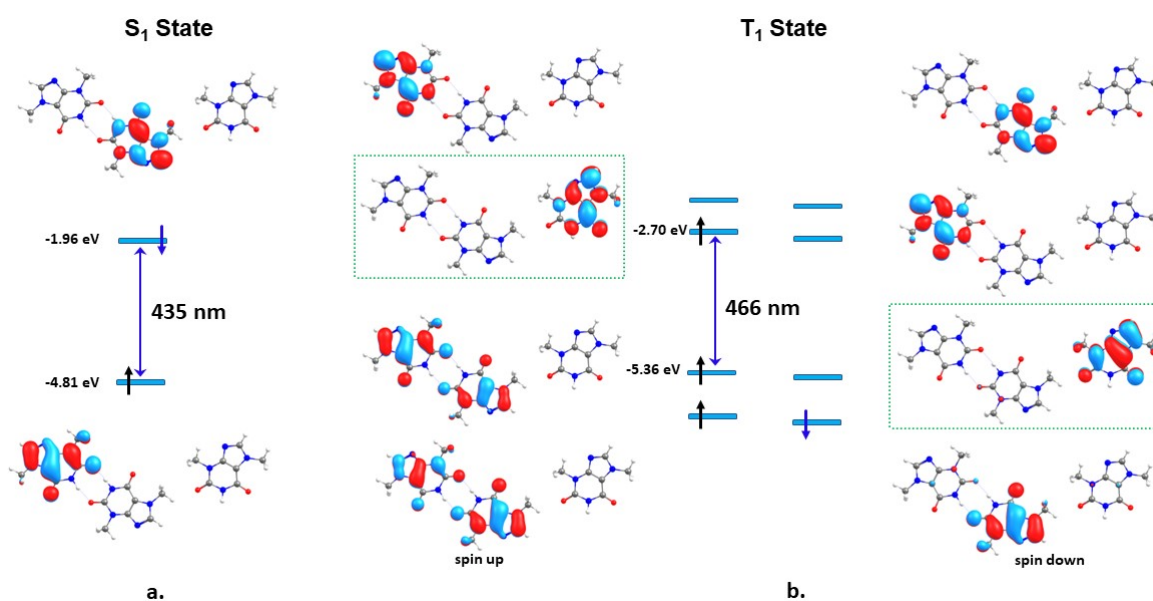


Figure S10. Frontier molecular orbitals of theophylline (TPH) based on the configurations of first electronic excited state. a. FMO of TPH in the S_1 electronic state. b. FMO of TPH in the T_1 electronic state. MO involved in these emissive states of the T_1 electronic state are dotted by green lines.

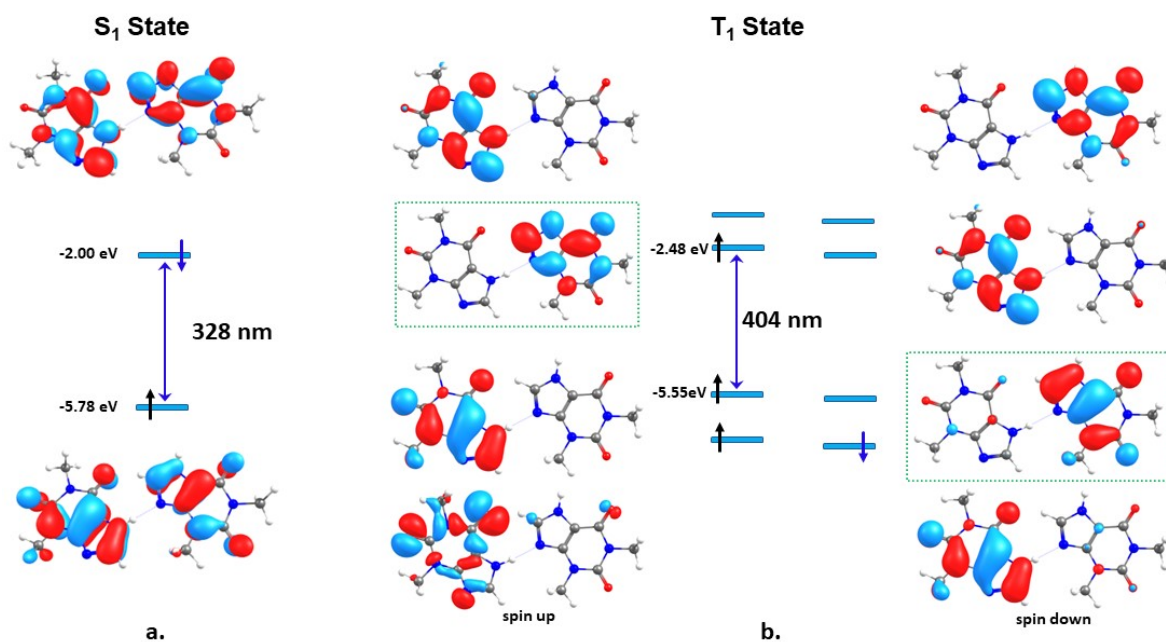


Figure S11. Frontier molecular orbitals of cocrystals based on the configurations of ground electronic excited state. a. FMO of CAF-DITFB in the S_0 electronic state. b. FMO of TPH-DITFB in the S_0 electronic state. c. FMO of TBR-DITFB in the S_0 electronic state.

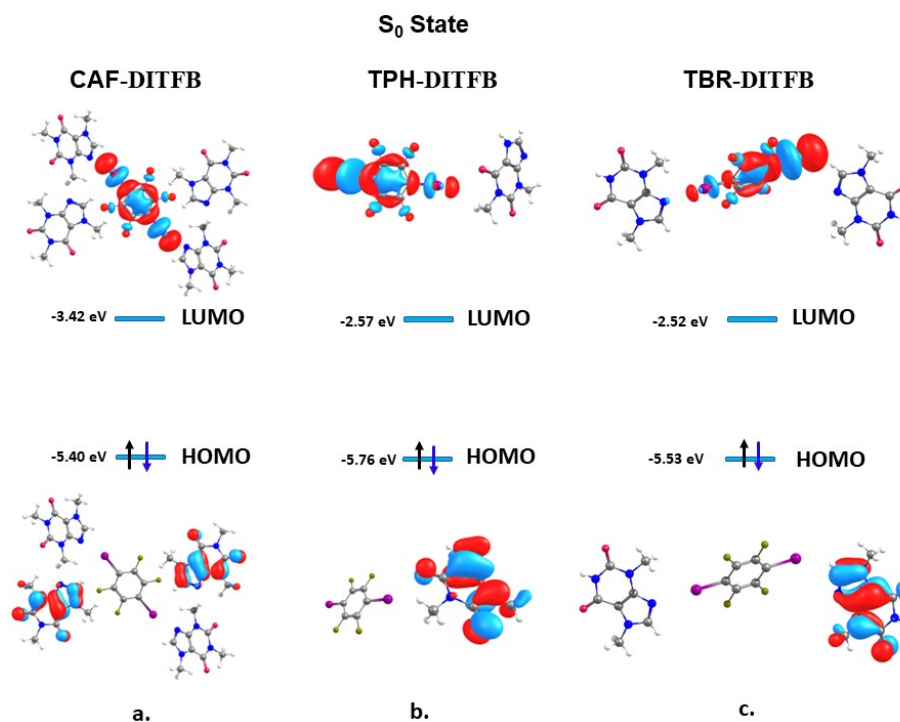


Figure S12. Energy diagrams for the most probable emission pathways in cocrystals. ISC, intersystem crossing.

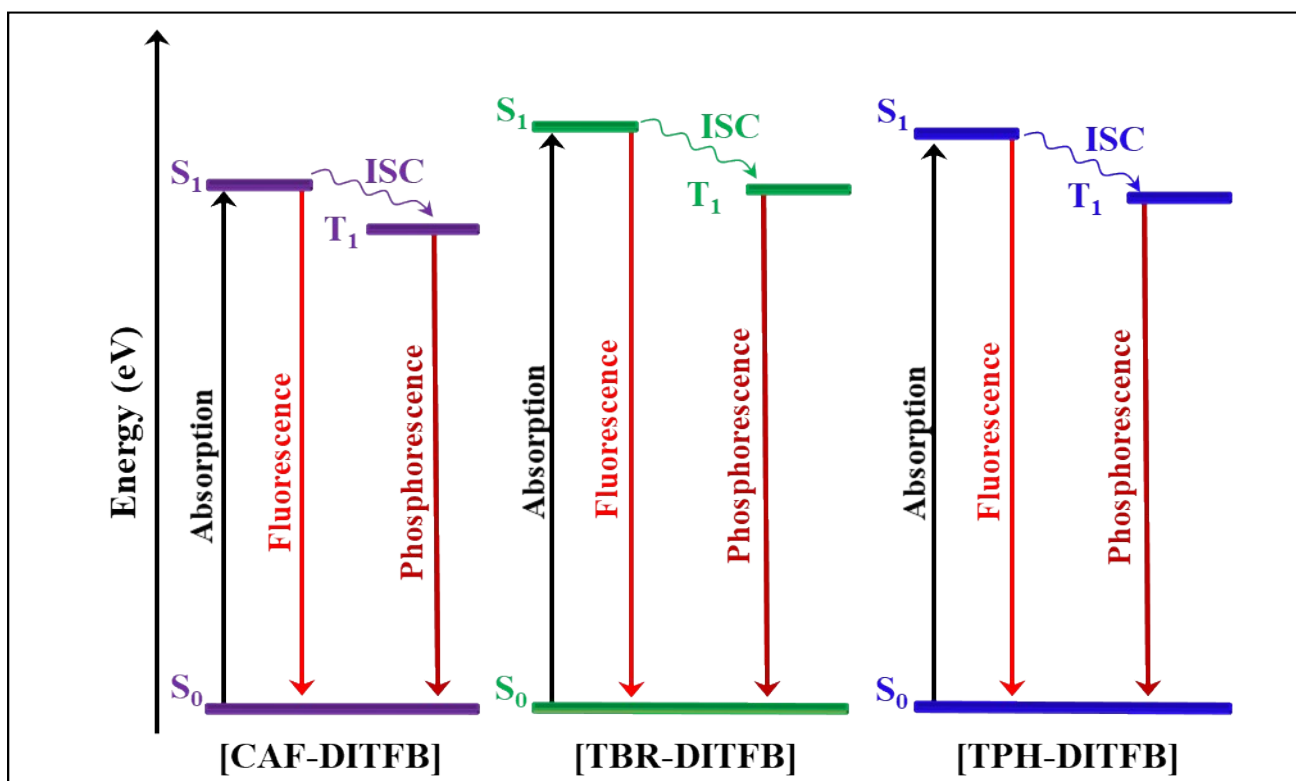


Figure S13. Frontier molecular orbitals of cocrystals **CAF-DITFB** based on the configurations of first electronic excited state. a. FMO of **CAF-DITFB** in the S_1 electronic state. b. FMO of **CAF-DITFB** in the T_1 electronic state. MO involved in these emissive states of the T_1 electronic state are dotted by green lines.

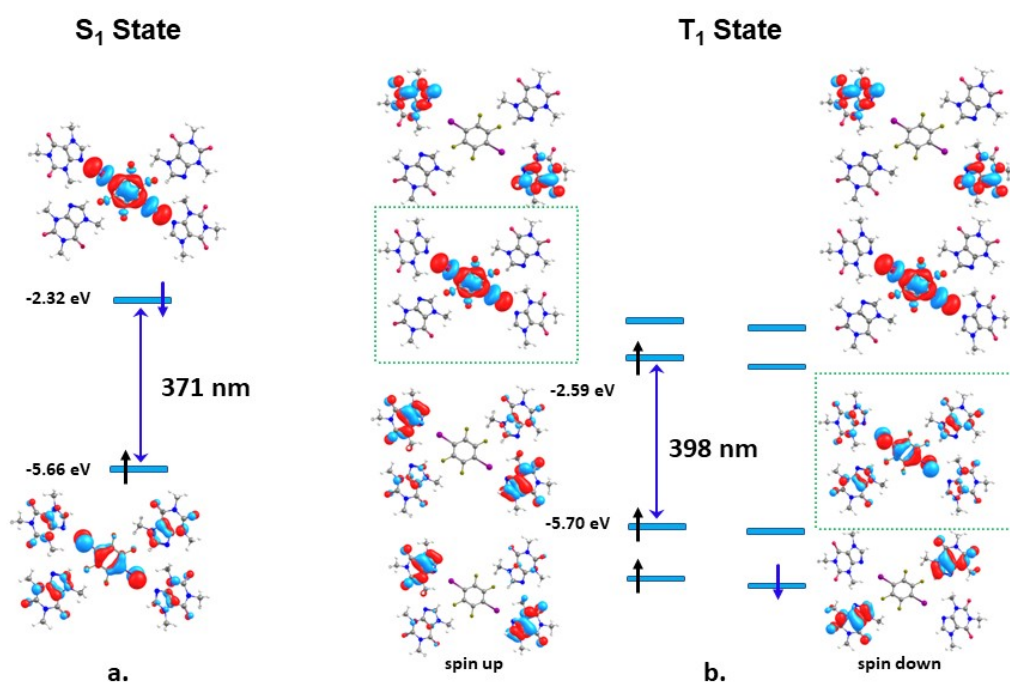


Figure S14. Frontier molecular orbitals of cocrystals **TPH-DITFB** based on the configurations of first electronic excited state. a. FMO of **TPH-DITFB** in the S_1 electronic state. b. FMO of **TPH-DITFB** in the T_1 electronic state. MO involved in these emissive states of the T_1 electronic state are dotted by green lines.

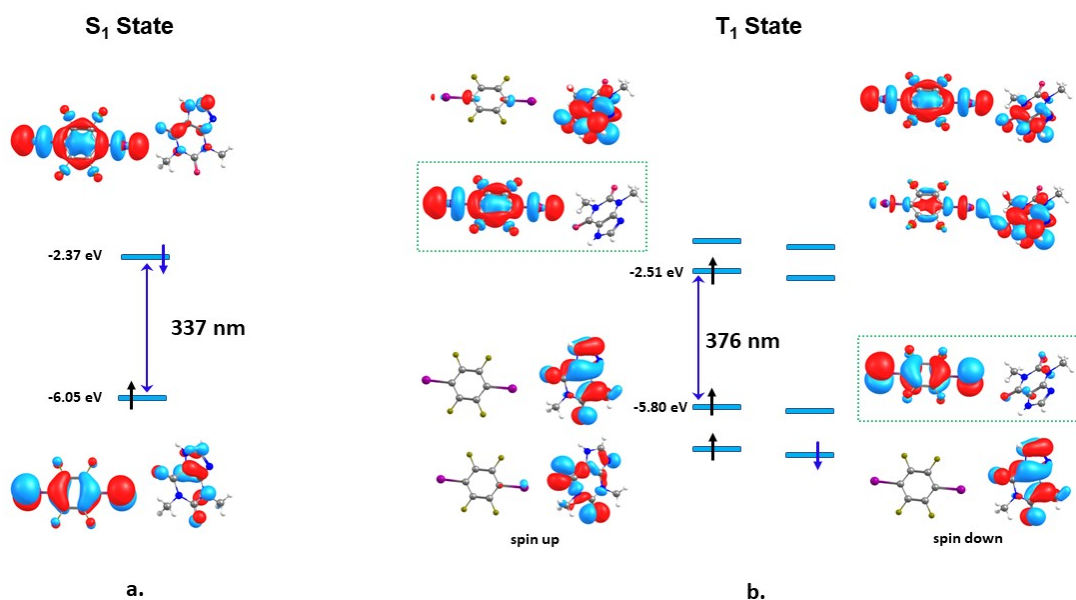


Figure S15. Frontier molecular orbitals of cocrystals **TBR-DITFB** based on the configurations of first electronic excited state. a. FMO of **TBR-DITFB** in the S_1 electronic state. b. FMO of **TBR-DITFB** in the T_1 electronic state. MO involved in these emissive states of the T_1 electronic state are dotted by green lines.

